Preprints (www.preprints.org) | NOT PEER-REVIEWED | Posted: 28 January 2018 doi:10.20944/preprints201801.0264.v1

Peer-reviewed version available at Energies 2018, 11, 590; doi:10.3390/en11030590

Article

Study on Hot Gases Flow in Case of Fire in a Road Tunnel

Aleksander Król [1,*] and Małgorzata Król [2]

[1] Faculty of Transport, Silesian University of Technology, Krasińskiego 8, 40-019 Katowice, Poland
[2] Faculty of Energy and Environmental Engineering, Silesian University of Technology, Konarskiego 18, 44-100 Gliwice, Poland, malgorzata.krol@polsl.pl
* Correspondence: aleksander.krol@polsl.pl; Tel.: +48-326-034-120

Abstract: This paper presents the results of hot smoke tests, conducted in a real road tunnel. The tunnel is located within the expressway S69 in southern Poland between cities Żywiec and Zwardoń. Its common name is Laliki tunnel. It is a bi-directional non-urban tunnel. The length of the tunnel is 678 m and it is inclined by 4%. It is equipped with the longitudinal ventilation system. Two hot smoke tests have been carried out according to Australian Standard AS 4391-1999. Hot smoke tests corresponded to a HRR (Heat Release Rate) equal to respectively 750 kW and 1500 kW. The fire source was located in the middle of the road lane imitating an initial phase of a car fire (respectively 150 m and 265 m from S portal). The temperature distribution was recorded during both tests using a set of fourteen thermocouples mounted at two stand poles located at the main axis of the tunnel on windward. The stand poles were placed at distances of 5 m and 10 m. The recorded data were applied to validate of a numerical model built and solved using Ansys Fluent. The calculated temperature distribution matched the measured values.

Keywords: road tunnel; fire; Ansys Fluent; smoke movement; temperature distribution

1. Introduction

The development of a fire in a road tunnel is always a huge threat. The appearance of large amounts of toxic smoke makes it very difficult to evacuate people and the operation of rescue teams. The limited space of the tunnel means that the rapidly increasing temperature is also a threat.

Evacuation of people from the tunnel should start as soon as possible. It begins after noting the fire - this applies to direct observers. However, it concerns all other endangered users of the tunnel only after activation of the fire emergency system. Activation of the fire system takes place after receiving a signal from a smoke detector, laser fiber sensor or tunnel technical service through video monitoring. The triggered fire signal activates sound and light systems that signal the necessity of evacuation. At the same time, the location where the signal was triggered informs the technical service and the emergency services about the place of fire development. This is of great importance for the operation of emergency services and for the activation of the fire ventilation system. Often, the fire ventilation system in the road tunnel is activated according to a specific emergency operation pattern, depending on the location of the fire. Such a working system is usually found in bidirectional tunnels. The safety of endangered people in the tunnel depends, to a large extent, on the speed of activation of the emergency system and the proper operation of the fire ventilation system under given conditions. During common daily operation of the tunnel, the fans are turned on for ventilation purposes or dilution of pollutants. The signal aroused by exceeding the permissible concentrations of traffic pollution or a decrease in visibility will cause the fans to switch on in the normal mode [1].

All road tunnels should be equipped with fire ventilation systems. Depending on the length of the tunnel and whether the road traffic is one or bidirectional, it can be equipped with longitudinal ventilation, transverse ventilation or semi-transverse ventilation. For tunnels up to 1000 meters long, longitudinal ventilation systems are most often designed. For longer tunnels, transverse ventilation

© 2018 by the author(s). Distributed under a Creative Commons CC BY license.

Preprints (www.preprints.org) | NOT PEER-REVIEWED | Posted: 28 January 2018 doi:10.20944/preprints201801.0264.v1

Peer-reviewed version available at Energies 2018, 11, 590; doi:10.3390/en11030590

is designed. The operation of longitudinal ventilation is based on the operation of axial fans located under the tunnel ceiling. A design of a longitudinal ventilation system involves determining the number and arrangement of axial fans.

The correct operation of longitudinal ventilation in a road tunnel is when the air accelerated by axial fans reaches the critical velocity and hot fumes are discharged through the nearest portal. In the initial growth phase of a fire, the critical velocity should be sufficient to ensure that both smoke and heat flow in the required direction. On the other hand, it should not disturb the natural stratification of smoke and air layers in the tunnel [2]. Smoke flow in the opposite direction is defined as backlayering. Backlayering can lead to complete smokiness of a tunnel. This phenomenon is strongly undesirable because it causes smoke to contaminate the entire tunnel despite the operation of the longitudinal ventilation [3]. Researchers are conducting a lot of studies to avoid this phenomenon during operation of fire ventilation. Gannouni used numerical analyses to study the impact of ventilation air velocity and the power of fire on the phenomenon of backlayering [4]. Studies on backlayering have shown that it can also occur locally in situations where the air velocity decreases near the tunnel walls or at its bend [5, 6]. On the other hand, Yao investigated the appearance of reverse smoke flow in tunnels with vertical ventilation ducts [7].

The basic requirement for properly operating fire ventilation in the tunnel is to generate a flow with a specified critical velocity. It turns out, however, that many factors affect the value of this velocity. The one of them is the inclination of a tunnel. It causes additional airflow related to the natural stack effect. It is assumed, that if the inclination is greater than 1 – 2%, this fact should be taken into account when designing the ventilation system and determining the critical velocity [8,9,10]. The natural stack effect can be strengthened by the action of the wind [11]. It is obvious that if the slope of the tunnel and the wind blowing outside the tunnel affect the critical velocity value, these factors will also affect the flow of smoke in the initial phase of the fire. It may happen that the fire does not outbreak at once with very high power and in the initial stage the smoke does not reach high temperatures. Smoke of a low temperature, in the initial phase of a fire can float just over the road surface. This will result in an uncontrolled flow of smoke and consequently a delayed activation of the fire emergency system.

Studying the phenomena occurring in the tunnel during the fire development is difficult. Both model studies [12-15] and numerical analyses [16-19] are used for this purpose. Many authors point to the lack of data from research in real tunnels, which could be the basis for the validation of numerical models [17,19]. Undoubtedly, numerical analyses are the cheapest and most willingly used way to study phenomena accompanying the development of fire and the operation of fire ventilation systems [20-23].

The numerical model of a road tunnel was presented in the article. The model was used to study the smoke flow in the tunnel under wind conditions. The model was validated using the results of tests carried out in a real road tunnel. The presented experimental research was actually wider and included the measurements of air flows too [11]. The article also presents a short description of the tunnel and tests with hot smoke.

2. Description of the tunnel

The tunnel is located on the S69 road and it links Żywiec and Zwardoń. The length of the tunnel is 678 m, the width is 11.9 m and the height is 6.55 m. The gradient (inclination) of the tunnel is 4%. The tunnel is not rectilinear (Figure 1). The northern portal has an elevation of 669 m a. s. l. and the southern portal has an elevation of 642 m a. s. l.

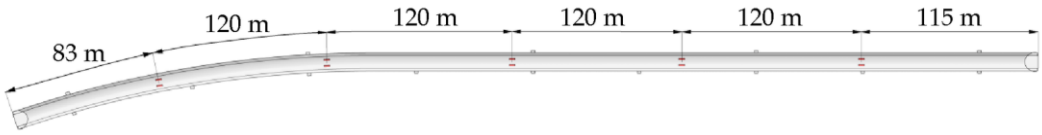

Figure 1. The overlay of the tunnel and location of the fans.

Preprints (www.preprints.org) | NOT PEER-REVIEWED | Posted: 28 January 2018 doi:10.20944/preprints201801.0264.v1

Peer-reviewed version available at Energies 2018, 11, 590; doi:10.3390/en11030590

The tunnel is divided into 5 sections, where the first is near the northern portal. Each section has two fans mounted. The emergency operation pattern of the fans is set up to activate them in a given section depending on the location of fire ignition. Figure 2 shows the division of the tunnel into sections and assignment of the fans. It presents also a part of the emergency operation pattern of the fans.

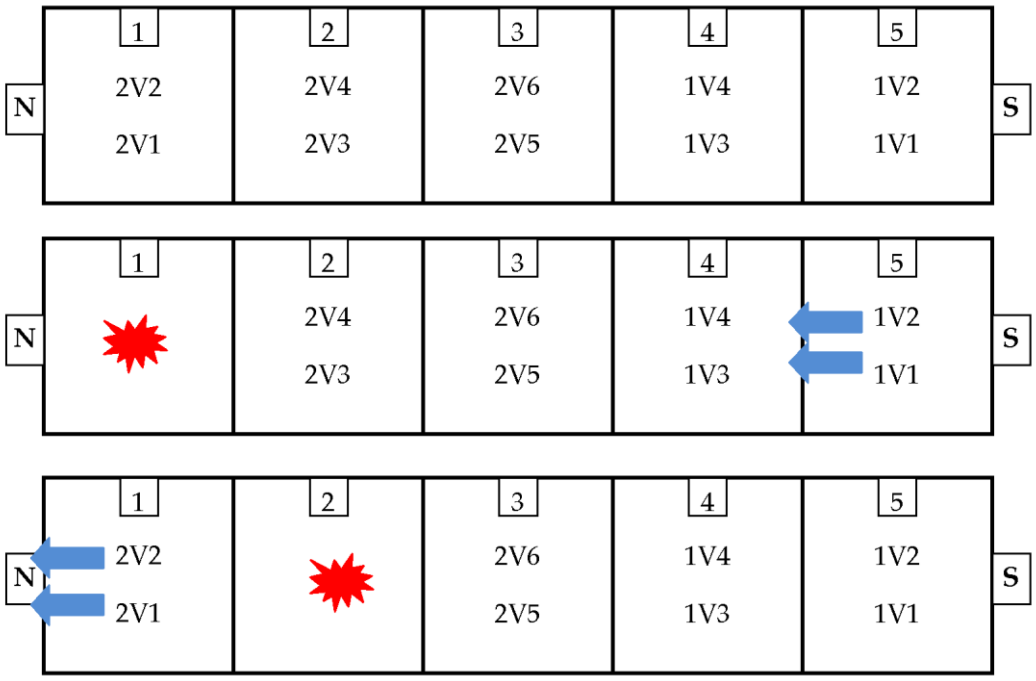

Figure 2. Sections in the tunnel. Dimensions are given in meters; the figure is not to scale.

The work of the fans was determined in such a way to avoid smokiness of whole the tunnel. The main rule was to remove smoke instead of allowing it to flow through the tunnel. For example, a fire in section 1 should initially activate fans 1V2 and 1V1 blowing in the N direction. A fire in section 2 should initially activate fans 2V2 and 2V1, also blowing in the N direction.

The fans can also work in normal mode. The fans will turn on when the concentration of harmful substances in the tunnel is exceeded or the visibility decreases. The direction of operation of the fans in the normal mode is consistent with the direction of the natural draught in that tunnel, i.e. S→N.

3. Experimental method

3.1. Air velocity measurements

Air velocity data was recorded by the ultrasonic gauge FLSE200H was taken into account for comparison purposes. The gauge manufactured by SICK MAIHAK Company was mounted under the tunnel ceiling at the distance of 114 from northern portal. Its measurement range was from -20 to 20 m/s with accuracy of ±0.1 m/s.

3.2. Hot smoke tests

Two hot smoke tests have been conducted. They were based on the Australian Standard AS 4391-1999 [24]. Five smoke generators made by the Vulcan Company and two or four fire trays (containing ethanol) were in use. According to the above standard, two fire trays of A1 size filled with 16 dm^3 of ethanol give a heat output (HRR) of 700 kW, whereas four fire trays the same size produce a heat output (HRR) of 1500 kW. Such trays configuration and the amount of fuel should

Preprints (www.preprints.org) | NOT PEER-REVIEWED | Posted: 28 January 2018 doi:10.20944/preprints201801.0264.v1

Peer-reviewed version available at Energies 2018, 11, 590; doi:10.3390/en11030590

assure the following sequence: 3 min of fire growth, 10 min of stable fire and 3 min of decay [24]. The trays were placed in the middle of the road lane (Figure 3).

Figure 3. Configuration of the generators and trays during both hot smoke tests (left – two trays, right – four trays).

Fourteen thermocouples, which were located at two pole stands, and a Flir thermo-vision camera, were used to determinate the temperature. The pole stands were located along the tunnel axis at distances of 5 m and 10 m from the final tray towards the S portal (Figure 4).

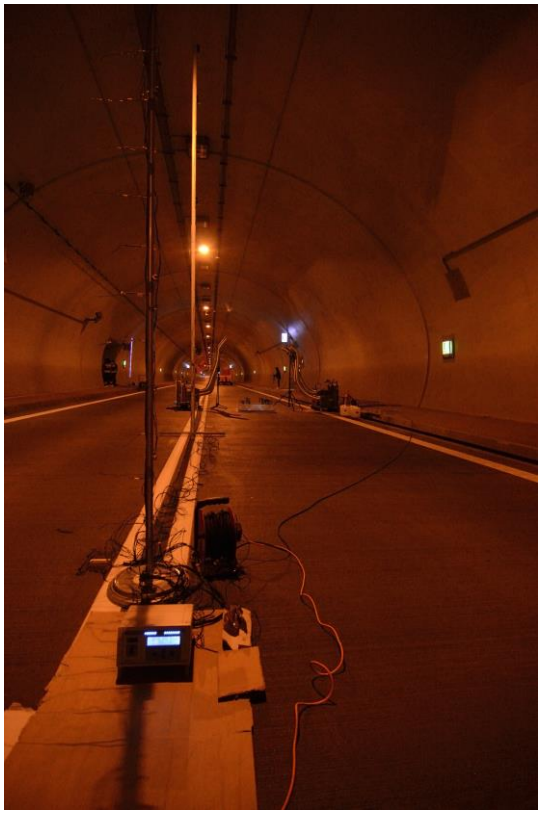

Figure 4. Pole stands with thermocouples and a thirty-channel thermometer.

The fans were turned on automatically in the first test. The details of the hot smoke test are given in Table 1.

Table 1. Hot smoke tests – details.

Test no.	Start hour	Location of measuring stand	Number of generators	Number of trays	Fuel

Preprints (www.preprints.org) | NOT PEER-REVIEWED | Posted: 28 January 2018 doi:10.20944/preprints201801.0264.v1

Peer-reviewed version available at Energies 2018, 11, 590; doi:10.3390/en11030590

1	17:17	150 m from S portal	5× Vulcan	2 × A1	Ethanol
2	18:10	265 m from S portal	5× Vulcan	4 × A1	Ethanol

4. Results

4.1. Ambient conditions during the tests

Wind strongly influences airflow and smoke flow in a tunnel (especially in a long one). Thus, wind velocity and direction were measured at both portals of the tunnel during the tests. An Ultrasonic anemometer WindMaster Pro, manufactured by Gill Instruments was used at the N portal. It allows for measurement of wind velocity in three dimensions by determination of particular vectors in 3D. However, only the horizontal velocity was taken into further consideration. The range was from 0 to 45 m/s. Accuracy was 1% RMS with resolution 0.01 m/s. The meteorological station Kestrel 4500 was used at the S portal. The range was from 0.4 to 40 m/s. Accuracy was 5% with resolution 0.1 m/s. Both devices were placed close to the portals to measure the actual wind parameters at the portals. The variations of wind velocity and wind direction during the tests are given in Table 2.

Table 2. The variations of wind velocity and wind direction during the tests.

	S portal		N portal	
Time	**Wind velocity [m/s]**	**Wind direction [˚]**	**Wind velocity [m/s]**	**Wind direction [˚]**
17:00	0.9	-124	0.7	-160
18:00	0.7	-131	0.3	-126
19:00	0.8	-118	0.4	-145

Direction 0˚ corresponds to wind from N, 90˚ to E, ±180˚ to S and -90˚ to W. The atmospheric pressure was 942 hPa and was almost unchanged during the whole day. The temperature was also stable and varied between 7°C and 8°C.

4.2. Hot smoke tests – temperature distribution

Two hot smoke tests were carried out. During the first test, two trays containing ethanol were burned and this provided an HRR equal to 700 kW, according to the Australian Standard [24]. Two pole stands with mounted thermocouples were in use. They were placed on windward, respectively 5 m and 10 m from the edge of the last tray. During the test, it turned out that the natural stack effect produced a strong natural airflow, forcing the smoke to flow almost horizontally (Figure 5) and no temperature increase at the thermocouples was detected.

Figure 5. Horizontal direction of smoke flow during the first hot smoke test.

Preprints (www.preprints.org) | NOT PEER-REVIEWED | Posted: 28 January 2018 doi:10.20944/preprints201801.0264.v1

Peer-reviewed version available at Energies 2018, 11, 590; doi:10.3390/en11030590

During the first test, the fire ventilation system was expected to turn on automatically. The first level of alarm was triggered in the 4th section instead of the 5th (Figure 6). The smoke was flowing towards the N portal due to the natural stack effect. The temperature of the smoke was low enough that the fire ventilation was not triggered. Ventilation system was switched on in normal mode because moving smoke caused a decrease of visibility. Hence, the visibility sensor gave a signal to start the ventilation system. As a result the fans started working in the 3rd section in the normal operation mode.

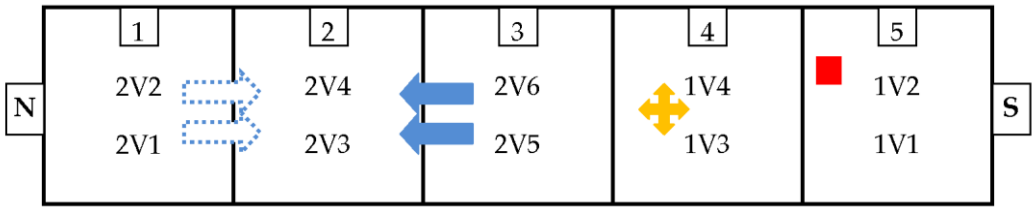

Figure 6. Operation pattern of fans with the operating status of devices during the test.

The location of the trays with burning ethanol is shown in Figure 6. The position of the visibility sensor in section 4th is also marked. The expected reaction of fire ventilation system is marked by dotted arrows, filled arrows shows the actual operation of the ventilation system in normal mode. As the trays with burning alcohol were located in 5th section, the proper fire detection should indicate the fire in this section. Therefore the fans in 1st section should be activated in the fire mode. However, eventually the fans were activated in the 3rd section in normal mode operation, what caused smokiness in whole tunnel.

Four trays were applied in the second test. This provided an HRR equal to 1500 kW according to the Australian Standard [24]. The location of the test point was also moved (see Table 1), although the configuration of pole stands was the same as during the first test. Considering the strong natural stack effect [11], it was decided to cover partially the portal S by a curtain. The curtain covered 90% of the cross-section area of S portal, so the natural draught was diminished to the value of 0.6 m/s. During the second test, automatic detection of fire ventilation was turned off. Then a temperature increase was detected. The temperature distribution at 5 m and 10 m is given in Figures 7 and 8.

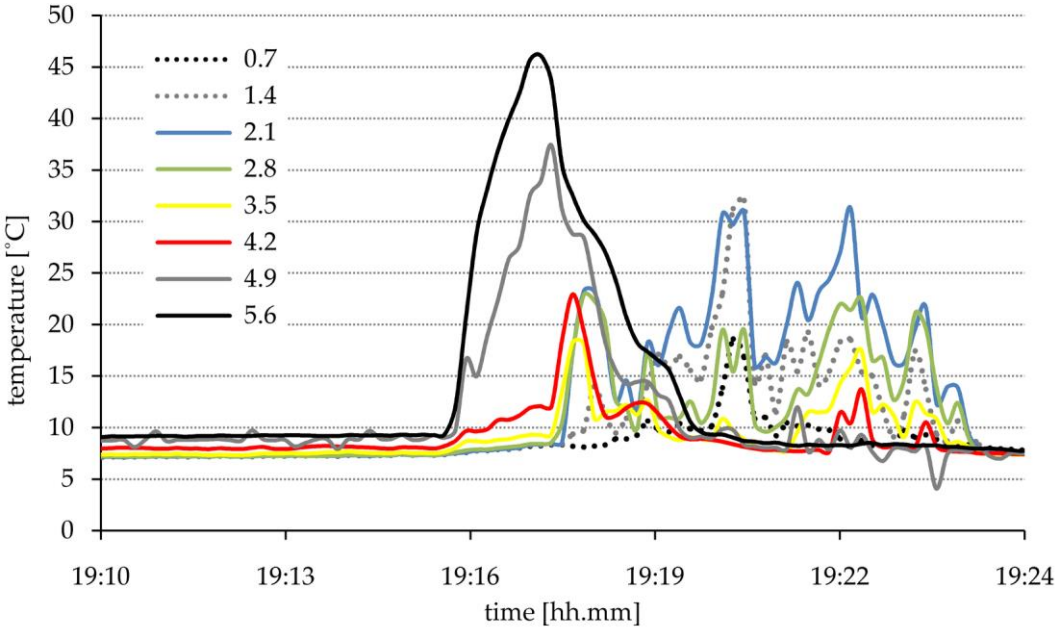

Figure 7. Temperature distribution on windward at 5 m from the last tray. The height of a measuring point is given in meters.

Preprints (www.preprints.org) | NOT PEER-REVIEWED | Posted: 28 January 2018 doi:10.20944/preprints201801.0264.v1

Peer-reviewed version available at Energies 2018, 11, 590; doi:10.3390/en11030590

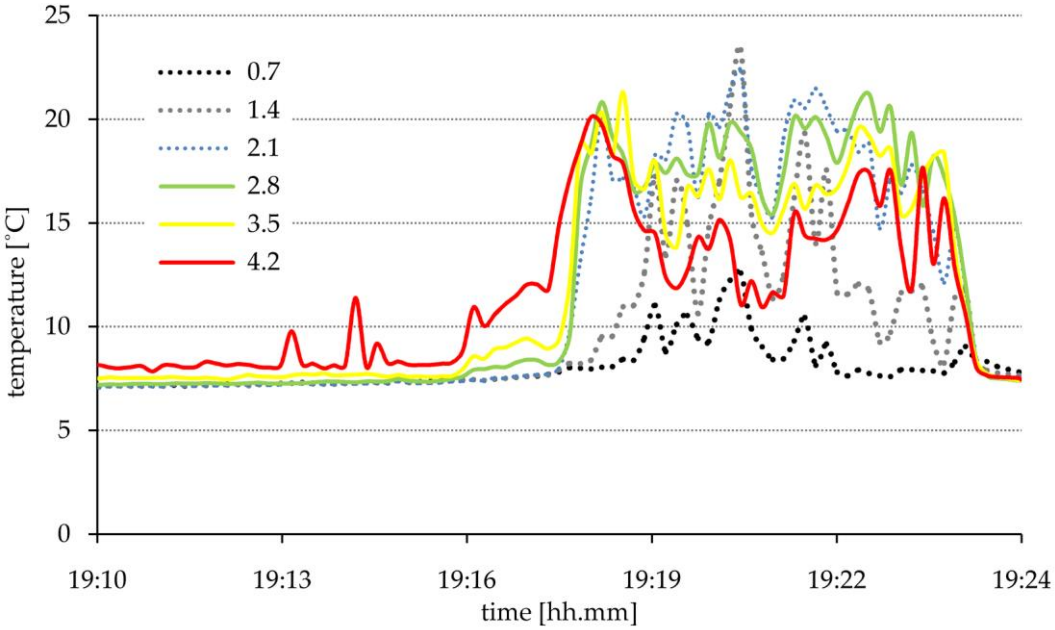

Figure 8. Temperature distribution on windward at 10 m from the last tray. The height of a measuring point is given in meters.

The second hot smoke test showed an increase of temperature on the windward side. A reading of 46°C was recorded at a height of 5.6 m, 5 meters from the final tray. Due to relatively short time of the hot smoke test, the tunnel ceiling was not warmed up significantly – the temperature of the tunnel ceiling just above the fire, as measured by the thermo-vision camera, did not exceed 20°C. As was already mentioned a residual natural flow remained, thus despite covering the S portal, smoke flow to the N portal was detected. Therefore, during this test, the leeward part of the tunnel was filled with smoke.

5. The numerical analysis of a fire development

5.1. Numerical modeling of combustion process

The process of combustion is a very complex phenomenon. It involves many chemical reactions between the components of the fuel and the oxidant which produce various intermediate and final products and release large amounts of energy. Complex turbulent flows must be also taken into account. This is a reason why some simplifications and pre-assumptions are required. The more so, because the research is focused on conditions inside the object in fire rather than on details of the combustion process. There are two fire models available when using Ansys Fluent software [25]:

- Species transport – the fire is modeled as a source emitting predefined combustion products. The mass flow rate and temperature of emitted species should be adjusted to fit the required fire heat release rate (HRR). This model requires only solving the additional transport equations for each taken into account specie. This approach omits entirely the details of combustion chemistry, thus it is unable to model the fire development controlled by ventilation.
- Non-premixed combustion – with the main assumption that chemical reactions of combustion run very quickly, therefore they can be regarded as immediate in comparison with the flows of all considered chemical compounds. This assumption allows for treating of the combustion products (intermediate or final) and released heat as depending only on local composition of gases mixture and its temperature.

5.2. Numerical model

Preprints (www.preprints.org) | NOT PEER-REVIEWED | Posted: 28 January 2018 doi:10.20944/preprints201801.0264.v1

Peer-reviewed version available at Energies 2018, 11, 590; doi:10.3390/en11030590

The model consists of a tube representing the tunnel. Due to simplification, the curvature of the tunnel was neglected, but its inclination of 4% was kept. Both portals were modeled as 'pressure outlet' boundary condition. The atmospheric pressure is generated using User Defined Function (UDF) according to the formula describing the pressure decrease with the height:

$$p = p_0 - \rho g h \quad (1)$$

Additionally, a dynamic pressure component was added to the pressure at southern portal to model the wind influence:

$$p_{dyn} = \frac{\rho v_{wind}^2}{2} \quad (2)$$

The chemical reaction of combustion of ethanol in atmospheric oxygen runs according to following expression:

$$C_2H_5OH + 3O_2 \rightarrow 2CO_2 + 3H_2O \quad (3)$$

Because the fire power in considered case was rather low and the fire development was controlled by amount of fuel, it is no need to analyze the details of combustion process. So the model of species transport was adopted. The net calorific value of ethanol is 27.2 MJ, therefore to obtain HRR equal to 1.5 MW 0.055 kg of ethanol must burned at a second. As the result of combustion process, according to reaction (3) 0.105 kg of CO_2 and 0.065 kg of H_2O is produced per second. Such values are assumed when defining the fire source as mass flow inlet. The temperature of emitted gases was so adjusted to achieve the required HRR. According to Australian Standard [24] the initial phase of fire growth should last about 3 min and this was confirmed qualitative using the thermo-vision camera during the tests. Therefore this fact was taken into account by applying an UDF, which controlled the amount of emitted combustion products in the relevant way.

Because of relatively low fire power, the effect of radiative heat transport can be neglected. It was checked with the use of thermo-vision camera. In such circumstances there was no radiation model used.

The quality of results of numerical modeling, especially when modeling fluid flows with RANS (Reynolds Averaged Navier-Stokes) approaches strongly depends on numerical mesh used. To assure the proper reproducing of the flows close to the fire the volume surrounding the fire and convective plume above was meshed with denser grid. Five inflation layers were added in the vicinity of the tunnel walls, ceiling and floor. The mesh was generated use the cut cell assembly method, what allowed for almost regular mesh. The mesh sensitivity of the model was checked in steady calculation mode. Figure 9 shows the comparison of the results for three meshes of different densities, which are described in Table 3.

Table 3. Preliminary test meshes.

Mesh	No of elements	No of nodes
Coarse	184980	189026
Medium	319799	324590
Fine	486257	494184

Preprints (www.preprints.org) | NOT PEER-REVIEWED | Posted: 28 January 2018 doi:10.20944/preprints201801.0264.v1

Peer-reviewed version available at Energies 2018, 11, 590; doi:10.3390/en11030590

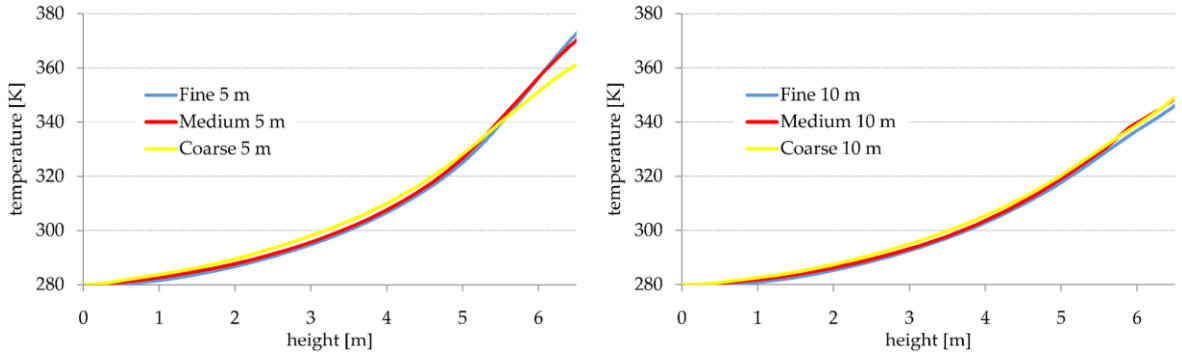

Figure 9. Temperature distribution at the tunnel axis on windward at 5 m and 10 m from the last tray for three mesh densities.

As it can be seen the results for medium and fine meshes were almost the same, thus the model with fine mesh can be regarded as mesh independent. Finally, the fine mesh was selected for successive calculations. Table 4 contains a summary of the numerical model.

Table 4. Numerical model summary.

Feature		Value
Turbulence model		*k*-omega SST
Fluid material		Air + CO_2 + H_2O (ideal gas)
Combustion model		Species transport
Fuel / combustion products		Ethanol C_2H_5OH / CO_2 + H_2O
Radiation model		none
Operating pressure		94200 Pa
Gravitational acceleration		9.81 m/s^2
Solver		Pressure based
Calculation mode		Transient
Time step		Adaptive (0.01 s – 0.1 s)
Pressure / velocity coupling		PISO
Under-relaxation factors	Pressure	0.2
	Momentum	0.2
	Energy	0.95
	Species	0.8
	Others	Default
Wall roughness		0.1 m

5.3. Numerical results and validation

The main aim of numerical analyzes was to reproduce the temperature distribution. Figure 10 and Figure 11 show the comparison of the measured temperatures with the calculated ones (the experimental data are the same as in Figures 7 and 8). The period of first 180 seconds of hot smoke test was taken into account. It was because in this period the fire developed in an undisturbed way (after then the fans were switched on manually to check the efficiency of smoke removal system).

Preprints (www.preprints.org) | NOT PEER-REVIEWED | Posted: 28 January 2018 doi:10.20944/preprints201801.0264.v1

Peer-reviewed version available at Energies 2018, 11, 590; doi:10.3390/en11030590

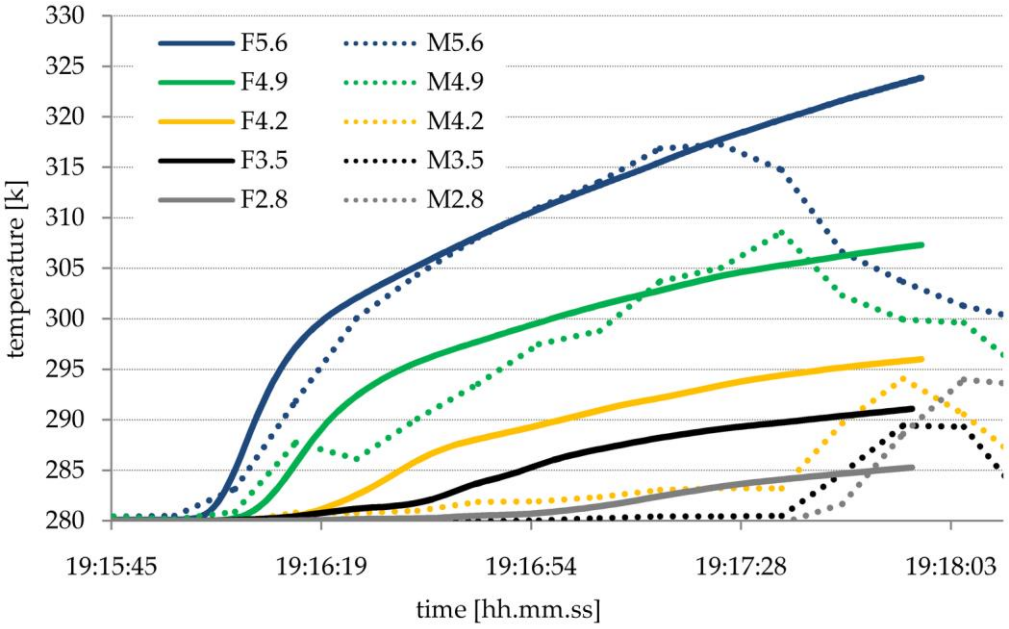

Figure 10. Temperature increase on windward at 5 m from the last tray. Prefix M denotes measurement, prefix F denotes Fluent calculation.

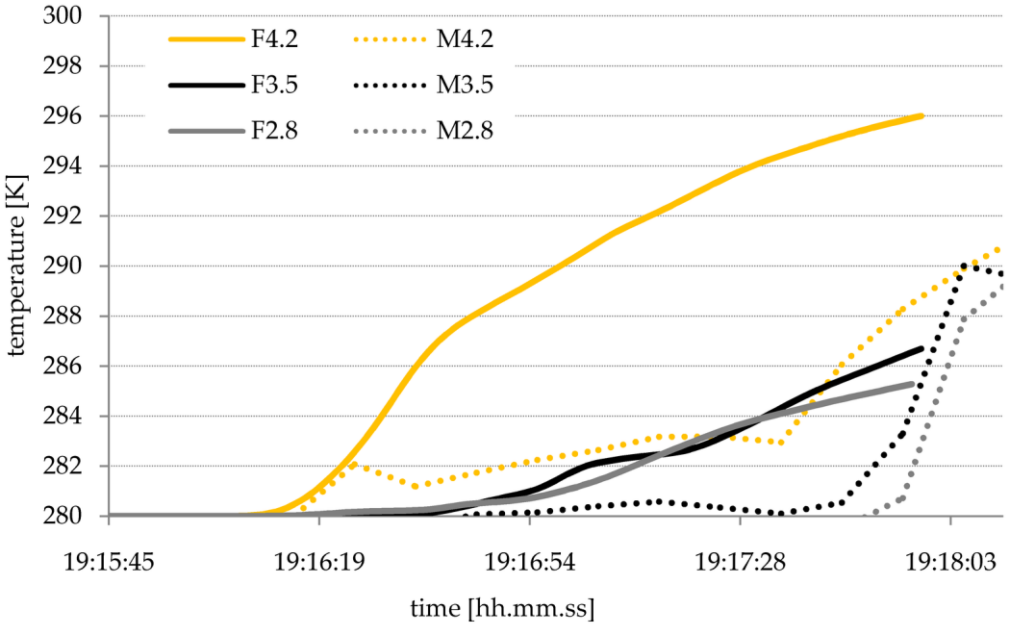

Figure 11. Temperature increase on windward at 10 m from the last tray. Prefix M denotes measurement, prefix F denotes Fluent calculation.

As it can be seen the results of numerical analyses agree with the measurements at least qualitatively. The temperature distribution and its variability in time are almost fully reproduced just under tunnel ceiling in close vicinity of the fire. It especially concerns the values of temperature measured by thermocouples mounted on the stand pole at the distance of 5 m from the last tray at the heights of 4.9 m and 5.6 m. It can be explained taking into account the fact that the buoyancy forces are significant there due to high temperature, so this portion of air is not susceptible to accidental gusts. Figure 12 shows the calculated temperature distributions in 160 second after the fire outbreak for two tunnel longitudinal cross-sections. The length of the shown tunnel section is about 114 m.

Preprints (www.preprints.org) | NOT PEER-REVIEWED | Posted: 28 January 2018 doi:10.20944/preprints201801.0264.v1

Peer-reviewed version available at Energies 2018, 11, 590; doi:10.3390/en11030590

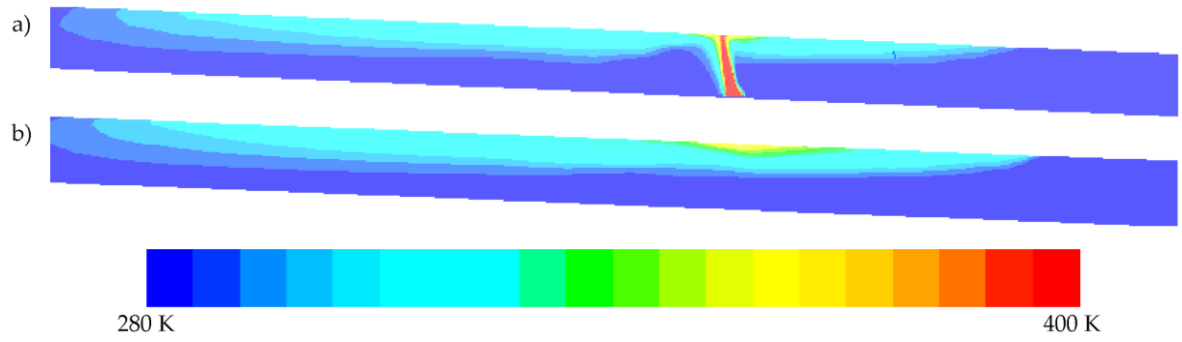

Figure 12. Temperature distributions in 160 second of fire development: a) at a plane of fire source, b) at the tunnel symmetry plane.

According to the expectations the gases moved towards the N portal because of the natural draught and the tunnel inclination. However, despite the relatively low fire power a portion of hot gases was able to move backward, what caused the measured temperature increase on windward. The extent of this backward movement of hot gases was estimated as about 20 m.

Figure 13 shows the calculated temperature distributions at the same time moment for two perpendicular tunnel cross-sections, which were located on both sides of fire source at a distance of 5 m. Worth noting is the fact that the point of the maximum temperature at the tunnel ceiling is not located just above the fire, but is shifted to the other side. This observation can be explained taking into account the velocity distribution shown in Figure 14.

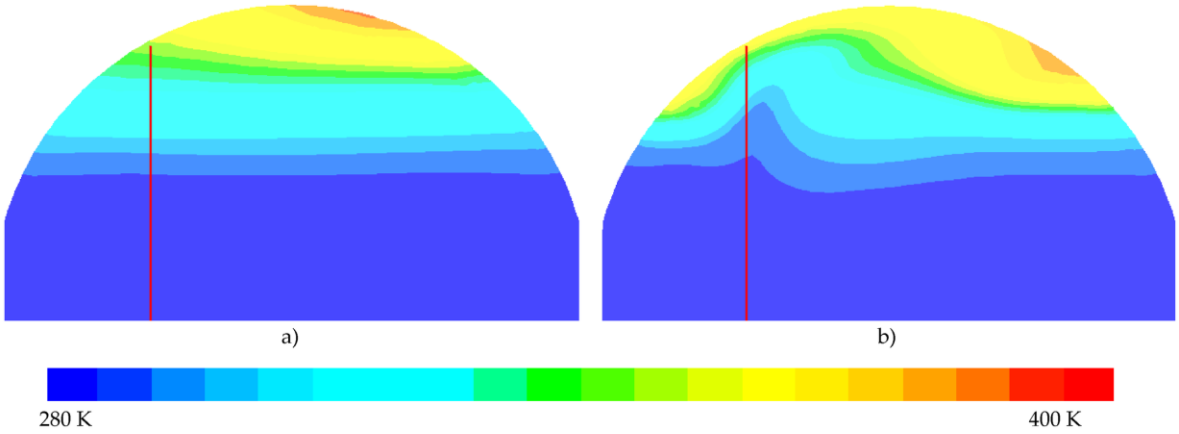

Figure 13. Temperature distributions in 160 second of fire development at two perpendicular cross-sections at a distance of 5 m from fire source: a) on windward, b) on leeward. The plane of fire source is marked

Preprints (www.preprints.org) | NOT PEER-REVIEWED | Posted: 28 January 2018 doi:10.20944/preprints201801.0264.v1

Peer-reviewed version available at Energies 2018, 11, 590; doi:10.3390/en11030590

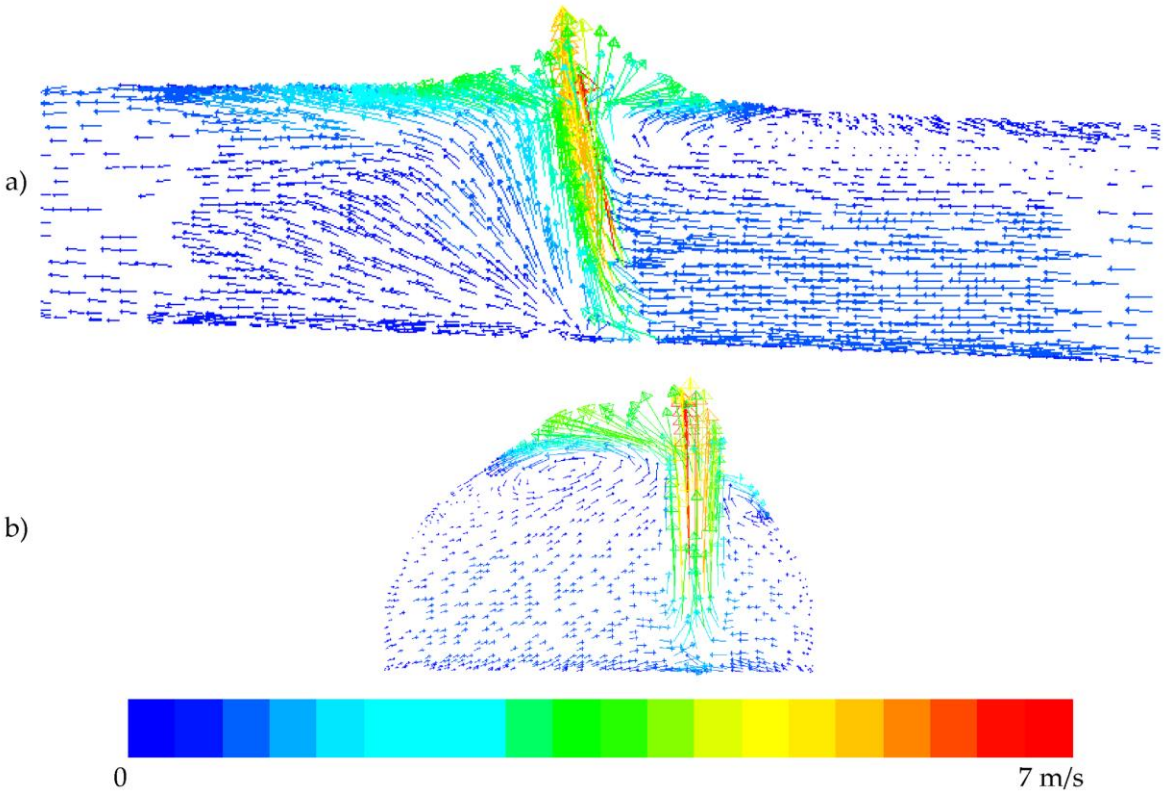

Figure 14. Visualization of velocity vectors in 160 second of fire development at two planes: a) at the plane of fire source, b) on a perpendicular cross-section at the leeward edge of trays.

As it can be observed the convective plume is slanted due to the natural draught. When the hot gases reached the ceiling they spread to both sides and flowed downward due to vault shape of the ceiling. Then, the downward movement was stopped by the buoyancy. It caused the accumulation of the hot gases at a distance beneath the ceiling. Additionally, the results of calculations showed that the fire caused the increase of the average longitudinal air velocity in the tunnel from about 0.60 m/s to 0.66 m/s.

6. Discussion and conclusions

The described studies and tests allowed for better understanding of phenomena which occurred in tunnels in a case of fire. Obviously, the hot smoke tests were limited by the fact that they were carried out during temporarily traffic shutdown in the real tunnel (commonly in a normal operation). Therefore, the maximum fire HRR was limited to 1500 kW, meanwhile according to British Standard [26] the heat flux of typical passenger car burning is 400 kW/m^2 and the area of fire is approximately 10 m^2, what gives 4000 kW for a fully developed fire. The average time of fire increase is about 10 minutes, but it varies in very wide range: between 5 and 15 minutes according to experiments [27]. Furthermore, the value of HRR for a truck in fire can reach up to 30 000 kW. However, as was mentioned in the Introduction section, the special attention must be paid to the initial phase of a fire development. This phase and the time factor are crucial taking into account the possibility of evacuation of threatened people. Thus, studies on low power fires which have just started to developed are very important because their results allow for assessing the conditions in a tunnel and the operation of live-saving systems. It was exactly the result of the first described test, which revealed the wrong operation of fire detection system.

The numerical analyses are nowadays willingly applied method of examining the operation of fire ventilation systems in tunnels. It is because the real tests are difficult to carry out. However, one should have in mind that numerical models without validation are not quite reliable. Despite the fact that the presented experiment was only a simulation of a real fire it gave a number of measured data,

Preprints (www.preprints.org) | NOT PEER-REVIEWED | Posted: 28 January 2018 doi:10.20944/preprints201801.0264.v1

Peer-reviewed version available at Energies 2018, 11, 590; doi:10.3390/en11030590

which were utilized for validation of numerical model. The presented results show that the model is validated correctly. Fire mapping in the numerical model seems to be accurate. The accordance of measured and calculated temperatures at a higher distance from the fire source looks worse, but the differences does not change the overall view of the situation. The numerical model validated by experimental data can be responsibly applied for further research on any fire configuration.

Acknowledgments: The authors would like to thank the General Directorate for National Roads and Motorways (Katowice Division) and the Headquarters of the State Fire Service in Katowice for the opportunity of conducting the research and for the management support provided. We would also like to thank the Smay Company and the Ardor Company for the technical support.

Author Contributions: Aleksander Król participated in the preparation of the research and took part in the research in the tunnel. He built a numerical model and carried out the numerical analyses. He participated in the writing of the article. Małgorzata Król took part in the planning and preparation of the research in the tunnel. She supervised the research and worked out the recorded data. She participated in the writing of the article.

Conflicts of Interest: The authors declare no conflict of interest. The founding sponsors had no role in the design of the study; in the collection, analyses, or interpretation of data; in the writing of the manuscript, and in the decision to publish the results.

References

1. NFPA 502. Standard for Road Tunnels, Bridges, and Other Limited Access Highways. **2011** Edition. Quincy: National Fire Protection Association
2. Klote, J.H.; Milke, J.A.; Turnbull, P.G.; Kashef, A.; Ferreira, M.J. Handbook of smoke control engineering. Atlanta, **2012**. GA: ASHRAE. ISBN 978-1-936504-24-4
3. Tang, F.; Li, L.J.; Mei, F.Z.; Dong, M.S. Thermal smoke back-layering flow length with ceiling extraction at upstream side of fire source in a longitudinal ventilated tunnel. *Appl. Therm. Eng.* **2016**, 106, 125–130. doi.org/10.1016/j.applthermaleng. 2016.05.173
4. Gannouni, S.; Maad, R.B. Numerical analysis of smoke dispersion against the wind in a tunnel fire. *J. Wind Eng. Ind. Aerodyn.* **2016**, 158, 61–68. doi.org/10.1016/j.jweia. 2016.09.009
5. Wang, F.; Wang, M. A computational study on effects of fire location on smoke movement in a road tunnel. *Tunn. Undergr. Space Technol.* **2016**, 51, 405–413. doi.org /10.1016/j.tust.2015.09.008
6. Wang, F.; Wang, M.; Carvel, R.; Wanga, Y. Numerical study on fire smoke movement and control in curved road tunnels. *Tunn. Undergr. Space Technol.* **2017**, 67, 1–7. doi.org /10.1016/j.tust.2017.04.015
7. Yao, Y.; Cheng, X.; Zhang, S.; Zhu, K.; Shi, L.; Zhang, H.; Smoke back-layering flow length in longitudinal ventilated tunnel fires with vertical shaft in the upstream. *Appl. Therm. Eng.* **2016**, 107, 738–746. doi.org/10.1016/j.applthermaleng.2016.07.027
8. Musto, M.; Rotondo, G. Numerical comparison of performance between traditional and alternative jet fans in tiled tunnel in emergency ventilation. *Tunn. Undergr. Space Technol.* **2014**, 42, 52-58. doi:org/10.1016/j.tust.2014.02.003
9. Chow, W.K.; Gao, Y.; Zhao, J.H.; Dang, J.F.; Chow, C.L.; Miao, L. Smoke movement in tilted tunnel fires with longitudinal ventilation. *Fire Saf. J.* **2015**, 75, 14-22. doi:org/10.1016/j.firesaf.2015.04.001
10. Lin, P.; Lo, S.M.; Li, T. Numerical study on the impact of gradient on semi-transverse smoke control system in tunnel, *Tunn. Undergr. Space Technol.* **2014**, 44, 68–79, doi.org /10.1016/j.tust.2014.07.011
11. Król, M.; Król, A.; Koper, P.; Wrona, P. Full scale measurements of the operation of fire ventilation in a road tunnel, *Tunn. Undergr. Space Technol.* **2017**, 70, 204–213, doi.org/10.1016/j.tust.2017.07.016
12. Wang, Y. F.; Sun, X. F.; Li, B.; Qin, T.; Liu, S.; Liu, Y. Small-scale experimental and theoretical analysis on maximum temperature beneath ceiling in tunnel fire with vertical shafts, *Appl. Therm. Eng.* **2017**, 114, 537–544. doi.org/10.1016/ j.applthermaleng.2016.12.040
13. Mei, F.; Tang, F.; Ling, X.; Yu, J. Evolution characteristics of fire smoke layer thickness in a mechanical ventilation tunnel with multiple point extraction, *Appl. Therm. Eng.* **2017**, 111, 248–256. doi.org/10.1016/j.applthermaleng.2016.09.064

Preprints (www.preprints.org) | NOT PEER-REVIEWED | Posted: 28 January 2018 doi:10.20944/preprints201801.0264.v1

Peer-reviewed version available at Energies 2018, 11, 590; doi:10.3390/en11030590

14. Tanaka, F.; Kawabata, N.; Ura, F. Effects of a transverse external wind on natural ventilation during fires in shallow urban road tunnels with roof openings, *Fire Saf. J.* **2016**, 79, 20–36. doi.org/10.1016/ j.firesaf.2015.11.004
15. Kashef, A.; Yuan, Z.; Lei, B. Ceiling temperature distribution and smoke diffusion in tunnel fires with natural ventilation, *Fire Saf. J.* **2013**, 62, 249–255. doi.org/10.1016/ j.firesaf. 2013.09.019
16. Eftekharian, E.; Dastan, A.; Abouali, O.; Meigolinedjad, J.; Ahmadi, G. A numerical investigation into the performance of two types of jet fans in ventilation of an urban tunnel under traffic jam condition, *Tunn. Undergr. Space Technol.* **2014**, 44, 56–67. doi.org /10.1016/j.tust.2014.07.005
17. Guo, X.; Zhang, Q. Analytical solution, experimental data and CFD simulation for longitudinal tunnel fire ventilation, *Tunn. Undergr. Space Technol.* **2014**, 42, 307–313. doi.org/10.1016/j.tust.2014.03.011
18. Wang, F.; Wang, M.; Wanga, Q. Numerical study of effects of deflected angles of jet fans on the normal ventilation in a curved tunnel, *Tunn. Undergr. Space Technol.* **2012**, 31, 80–85. doi.org/10.1016/j.tust. 2012.04.009
19. Cascetta, F.; Musto, M.; Rotondo, G.; Innovative experimental reduced scale model of road tunnel equipped with realistic longitudinal ventilation system, *Tunn. Undergr. Space Technol.* **2016**, 52, 85–98. doi.org/10.1016/j.tust.2015.11.025
20. Dziurzyński, W.; Krach, A.; Pałka, T. Airflow Sensitivity Assessment Based on Underground Mine Ventilation Systems Modeling; *Energies* **2017**, 10, 1451; doi:10.3390/en10101451
21. Chow, W.K.; Dang, J.F.; Gao, Y.; Chow, C.L. Dependence of flame height of internal fire whirl in a vertical shaft on fuel burning rate in pool fire, *Appl. Therm. Eng.* **2017**, 121, 712–720. doi.org/10.1016/ j.applthermaleng.2017.04.108
22. Węgrzyński, W. Transient characteristic of the flow of heat and mass in a fire as the basis for optimized solution for smoke exhaust, *Int. J. Heat Mass Transf.* **2017**, 114, 483–500. doi.org/10.1016/j.ijheatmasstransfer. 2017.06.088
23. Węgrzyński, W., Krajewski, G. Influence of wind on natural smoke and heat exhaust system performance in fire conditions. *J. Wind Eng. Ind. Aerodyn.* **2017**, 164, 44–53. doi.org/10.1016/j.jweia.2017.01.014
24. AS 4391 – **1999** Australian Standard Smoke management systems – Hot smoke test
25. Ansys Fluent Tutorial Guide, Ansys Inc., **2009**.
26. BS 7346-4 – Components for smoke and heat control systems. Part 4: Functional recommendations and calculation methods for smoke and heat exhaust ventilation systems, employing steady-state design fires – Code of practice, **2003.**
27. Jannsens M., Development of a database of full-scale calorimeter tests of motor vehicle burns, Southwest Research Institute, San Antonio Texas, **2008.**